




Older age, male sex, and cerebral microbleeds predict white matter loss after traumatic brain injury

David J. Robles · Ammar Dharani · Kenneth A. Rostowsky ·
Nikhil N. Chaudhari · Van Ngo · Fan Zhang · Lauren J. O'Donnell ·
Lauren Green · Nasim Sheikh-Bahaei · Helena C. Chui · Andrei Irimia 

Received: 12 August 2021 / Accepted: 11 September 2021 / Published online: 26 October 2021
© The Author(s), under exclusive licence to American Aging Association 2021

Abstract Little is known on how mild traumatic brain injury affects white matter based on age at injury, sex, cerebral microbleeds, and time since injury. Here, we study the fractional anisotropy of white matter to study these effects in 109 participants aged 18–77 (46 females, age $\mu \pm \sigma = 40 \pm 17$ years) imaged within ~ 1 week and ~ 6 months post-injury. Age is found to be linearly associated with white

matter degradation, likely due not only to injury but also to cumulative effects of other pathologies and to their interactions with injury. Age is associated with mean anisotropy decreases in the corpus callosum, middle longitudinal fasciculi, inferior longitudinal and occipitofrontal fasciculi, and superficial frontal and temporal fasciculi. Over ~ 6 months, the mean anisotropies of the corpus callosum, left superficial frontal fasciculi, and left corticospinal tract decrease significantly. Independently of other predictors, age and cerebral microbleeds contribute to anisotropy decrease in the callosal genu. Chronically, the white matter of commissural tracts, left superficial frontal fasciculi, and left corticospinal tract degrade appreciably, independently of other predictors. Our findings suggest that large commissural and intra-hemispheric structures are at high risk for post-traumatic degradation. This study identifies detailed neuroanatomic substrates consistent with brain injury patients' age-dependent deficits in information processing speed, interhemispheric communication, motor coordination, visual acuity, sensory integration, reading speed/comprehension, executive function, personality, and memory. We also identify neuroanatomic features underlying white matter degradation whose severity is associated with the male sex. Future studies should compare our findings to functional measures and other neurodegenerative processes.

D. J. Robles · A. Dharani · K. A. Rostowsky ·
N. N. Chaudhari · V. Ngo · A. Irimia (✉)
Ethel Percy Andrus Gerontology Center, Leonard Davis
School of Gerontology, University of Southern California,
Los Angeles, CA 90089, USA
e-mail: irimia@usc.edu

F. Zhang · L. J. O'Donnell
Department of Radiology, Brigham and Women's
Hospital, Harvard Medical School, Boston, MA 02115,
USA

L. Green · N. Sheikh-Bahaei · H. C. Chui
Department of Neurology, Keck School of Medicine,
University of Southern California, Los Angeles,
CA 90033, USA

N. Sheikh-Bahaei
Department of Radiology, Keck School of Medicine,
University of Southern California, 1520 San Pablo Street,
Los Angeles, CA 90033, USA

A. Irimia
Corwin D. Denney Research Center, Department
of Biomedical Engineering, Viterbi School of Engineering,
University of Southern California, Los Angeles,
CA 90089, USA

Keywords Diffusion tensor imaging · Fractional anisotropy · Susceptibility-weighted imaging · Sensory integration · Executive function

Introduction

Traumatic brain injuries (TBIs) are brain function disruptions caused by physical impacts leading to neural tissue damage. In industrialized countries, TBIs' burden on healthcare systems parallels the growing number of aging adults [1]. Even in mild TBI (mTBI), injury effects can be profound and long-lasting because TBI accelerates brain aging while increasing the risk for neurodegenerative diseases like Alzheimer's dementia. Every year, ~2.8 million Americans experiencing TBIs seek medical attention, with substantial age and sex disparities among them. Whereas males are more commonly affected [2], older adults' TBI vulnerability translates into their poorer clinical outcomes compared to all other age groups [3–5]. Because these outcomes reflect neural and cognitive deficits, delineating how sex- and age-related brain connectivity changes drive these deficits could help to inform future strategies for the mitigation of TBI sequelae.

The Glasgow Coma Scale (GCS) categorizes TBIs as mild, moderate, or severe, and mTBIs account for 70–90% of all cases [6, 7]. In acute geriatric TBI, susceptibility-weighted imaging (SWI, a type of magnetic resonance imaging sensitive to ferromagnetic compound deposits) frequently reveals cerebral microbleeds (CMBs, biomarkers of blood–brain barrier breakdown). CMB incidence increases with age due to blood vessel stiffening and to increases in blood–brain barrier permeability, both phenomena contributing to CMB risk [8]. Aside from occurring more frequently after geriatric mTBI, CMBs can be associated with persistent brain circuitry abnormalities, including white matter (WM) degradation. Although age and sex modulate such degradation, the relationship between CMBs and WM trajectories is largely unknown [9]. Understanding this relationship could help to reduce disparities in the neurocognitive outcome as a function of sex, age, CMB findings, and mTBI stage. Furthermore, quantifying the statistical effects of the latter factors upon WM degradation can complement our understanding of how neurophysiological, cognitive, and affective TBI sequelae are underlain by brain circuitry.

The first aim of this cohort study is to assess, across the first ~6 months post-injury, the statistical effects of age at injury, sex, and CMBs on fractional anisotropy (FA), a diffusion MRI measure reflecting WM properties. For major WM structures, we investigate how sex, age at injury, and CMBs predict mean FA at the acute and chronic stages of mTBI (within ~7 days and ~6 months post-injury, respectively). Our second aim is to study whether mean FA decreases significantly across the follow-up period above and beyond the effects of age, sex, and CMBs. We highlight how these variables modulate WM changes and explore how the latter may reflect the most common neurophysiological, cognitive, and affective outcomes of TBI patients. This is the first study to explore, in a systematic fashion, how age at injury, sex, CMBs, and their statistical interactions contribute to post-traumatic WM degradation.

Materials and methods

Study design and participants

This study was undertaken in adherence to the US Code of Federal Regulations (45 CFR 46) and with approval from the Institutional Review Board at the University of Southern California. Participants were recruited through community outreach via advertisements and flyers and/or with the assistance of healthcare professionals who had referred volunteers for neuroimaging and neurocognitive assessments. All subjects who satisfied inclusion criteria and who could provide written informed consent were invited to participate. Inclusion criteria included (1) an acute GCS score of at least 13 upon initial evaluation ($\mu \pm \sigma = 14 \pm 1$), (2) MRIs acquired within ~1 week and ~6 months post-injury, (3) a TBI related to a ground-level fall involving direct head trauma, (4) loss of consciousness (LOC) shorter than 30 min ($\mu \pm \sigma \approx 9 \pm 4$ min), and (5) post-traumatic amnesia shorter than 24 h ($\mu \pm \sigma \approx 3.6 \pm 2.1$ h). Exclusion criteria included (1) imaging findings other than CMB-related SWI hypointensities and (2) a documented clinical history of pre-traumatic neurological disease, psychiatric disorder, or drug/alcohol abuse. Cases of larger intracranial hemorrhage identified from SWIs were excluded. A total of 109 mTBI participants (46 females; age $\mu = 40.2$ years (y), $\sigma = 16.7$ y, range: 18–79 y) were included.

Neuroimaging

Two sets of magnetic resonance imaging (MRI) scans were acquired acutely (~ 7 days) and at ~ 6 months follow-up after injury. T_1 MRIs were acquired using a 3D magnetization-prepared rapid acquisition gradient echo sequence [repetition time (T_R)=1950 ms; echo time (T_E)=2.98 ms; inversion time (T_I)=900 ms; voxel size=1.0 mm \times 1.0 mm \times 1.0 mm]. T_2 MRIs were acquired using a 3D sequence (T_R =2500 ms; T_E =360 ms; voxel size=1.0 mm \times 1.0 mm \times 1.0 mm). Flow-compensated SWI volumes were acquired axially (T_R =30 ms; T_E =20 ms; voxel size=1.33 mm \times 1.33 mm \times 1.6 mm). Diffusion-weighted images (DWIs) were acquired axially in 64 gradient directions (T_R =8,300 ms; T_E =72 ms; voxel size=2.7 mm \times 2.7 mm \times 2 mm). Scans were de-identified and de-linked to preserve participants' confidentiality.

Preprocessing

DWIs were processed using 3DSlicer. DTIPrep was used with default parameters to correct eddy current and patient motion artifacts. Brain masks were created from DWI using SlicerDMRI. BRAINSFit was used for affine registration of both skull-stripped DWIs and B_0 volumes to T_1 volumes. Tractography was performed using unscented Kalman filter (UKF) two-tensor tractography and whole-brain seeding, with one seed per voxel and default parameters. UKF tractography is a deterministic fiber tracking method that fits two tensors at each step while tracking. Unlike single tensor deterministic tractography, where voxels are treated as independent and pathways are reconstructed by tracking in the direction of the principal eigenvector, two-tensor UKF tractography uses information from previous positions to guide model estimation and tracking at the current position. UKF tractography is very consistent in tracking fibers based on diffusion MRI data from independent samples across ages, health conditions, and image acquisitions [10]. FAs were calculated from UKF-derived tensors.

CMB identification

At least three expert raters with training in CMB identification found and segmented each CMB on SWI. CMBs were defined as small, intraparenchymal, round/ovoid SWI hypointensities distinct from blood vessels. Hypointensities connected to the exterior boundary of the brain were not labeled because CMBs are not connected to meninges. CMB labeling discrepancies were resolved by consensus. The distance between each cortical mesh vertex and the closest CMB was calculated for each subject, and this distance was plotted on the cortical surface. Such cortical maps were transformed to a common average template (atlas) and averaged over subjects to generate an average map of expected CMB proximities.

Cortical reconstruction and WM analysis

Automatic T_1 MRI segmentation was applied in FreeSurfer 6.0 (<https://surfer.nmr.mgh.harvard.edu/>) with default parameters. FreeSurfer (A) strips non-cortical voxels using a hybrid-watershed deformation procedure, (B) normalizes image intensities, (C) registers images into Talairach space, (D) segments WM and gray matter (GM), (E) tessellates the WM/GM boundary, and (F) corrects topological inaccuracies. WM parcellation was performed using an anatomically curated fiber clustering pipeline [11]. Input tractography data were affinely registered to the O'Donnell Research Group tractography atlas (<http://dmri.slicer.org/atlasses/>). WM tracts were identified automatically in each subject using the WM Analysis (WMA) package. WMA uses machine learning to identify subjects' WM tracts based on neuroanatomist-curated WM atlas. The atlas contains 58 deep WM tracts including major long-range association and projection tracts, commissural tracts, tracts related to the brainstem and cerebellar connections, and 198 short- and medium-range superficial fiber clusters organized into 16 categories according to the brain lobes that they connect. The left and right cortico-ponto-cerebellar tracts were treated as a single structure. Potential false positive tracts were annotated automatically to filter out outlier fibers. The mean FA of each WM structure was calculated.

Feature selection

Data dimensionality was reduced using a strategy proposed by Jolliffe [12, 13, 14] and adapted to our needs. Specifically, the mean FAs of each WM structure were assembled in an $N \times M$ matrix ($N = 109$ and $M = 73$ are the number of subjects and structures, respectively). A principal component analysis (PCA) with varimax rotations was applied to this matrix to identify the proportion of variance explained by each PC, which weighted each WM structure's contribution to the total variance. PCs were sorted in decreasing order by their explained variance, and PCs which together accounted for at least 50% of the variance were retained. Each retained PC was inspected to determine which WM structures' PC weights had the largest magnitude, and only those structures were retained. Thus, WM structures were retained based on PC weight magnitudes, subject to the constraint that both left and right portions of each structure had to have relatively large magnitudes. Thus, if a structure had a large magnitude for the left—but not for the right—hemisphere, the structure in question was not retained. By contrast, if a structure's left and right portions both had relatively large magnitudes, the structure was retained. This strategy ensured that only WM structures affected by TBI *bilaterally* were retained. This allowed us to investigate *global*—rather than *unilateral*—TBI effects. Whereas the latter can be of interest, their existence is more confounded by primary injury location. In samples like ours, unilateral effects are more likely driven by focal injury location rather than by the greater global vulnerability of WM structures to injury. It was also deemed judicious to focus on bilateral changes in WM fasciculi partly because (1) no information on primary injury locations (e.g., accelerometry data and neurological examinations) was available and (2) such information could confound our data in ways we could not quantify. After statistical feature selection, the seven Witelson subdivisions of the corpus callosum (CC) were combined based on whether they belonged to the genu (GCC), body (BCC), or splenium (SCC), thus reducing the number of CC structures in the analysis from seven to three. This was done to facilitate interpretation of results and comparison with previous studies, which typically describe findings pertaining to the GCC, BCC, and/or SCC rather than to Witelson subdivisions.

Analysis 1

We examined the relationship between sex, age, and CMB count, on the one hand, and WM mean FA, on the other hand. The mean FAs of the left and right parts of the WM structures of interest were included as a set of bivariate outcomes in a multivariate analysis of variance (MANOVA) whose independent variables were the participants' ages, sexes, and CMB counts. The omnibus null hypothesis stated that both bivariate regression coefficients are identically equal to zero, i.e., that there is no statistical relationship between the mean FAs of the left and right WM structures, on the one hand, and participants' ages, sex, and CMBs counts, on the other hand. We explored each predictor's contribution to the multivariate main effect, above and beyond all other predictors' contributions. Data associated with the first (i.e., acute) and second (i.e., chronic) time points were analyzed separately. The null hypothesis was tested at $\alpha = 0.05$. Both confidence intervals (CIs) for test statistics and p -values were computed. Effect sizes were assessed using Cohen's η^2 , and *post-hoc* statistical power was estimated.

Analysis 2

We implemented a repeated-measures MANOVA where age, sex, and CMB counts (independent variables) predicted mean FA changes (dependent variables) within the left and right portions of each WM structure. We used Hotelling's T^2 test for paired multivariate samples to identify WM structures whose mean FAs changed significantly by testing the omnibus null hypothesis of no mean FA change within each WM structure. Like in analysis 1, test statistics, CIs, p -values, Cohen's η^2 , and *post-hoc* statistical power were calculated.

Analysis 3

Using MANOVA, we investigated whether each predictor (age, sex, or CMB count) contributed significantly, above and beyond all other predictors, to mean FA changes within WM structures.

Results

Feature selection

Three PCs were retained because their sum was sufficient to explain ~50% of the mean FA variance (PC_1 : 39.6%; PC_2 : 5.3%; PC_3 : 4.7%). Our feature selection strategy identified ten WM structures for analysis: the GCC, BCC, SCC, inferior longitudinal fasciculus (ILF), middle longitudinal fasciculus (MdLF), inferior occipitofrontal fasciculus (IOFF), the corticospinal tract (CST), as well as superficial frontal (Sup-F), parietal (Sup-P), and temporal (Sup-T) fasciculi.

CMB locations

After computing the distance between each cortical mesh vertex and the closest CMB, this distance was plotted on the cortical surface for each subject and results were averaged across subjects to generate an average map of expected CMB proximities. This map (Fig. 1) revealed that, on average, CMBs could be localized close to the cortical

surface within (A) the lateral and medial aspects of the frontal and parietal lobes, (B) orbitofrontal cortex, (C) the left medial temporal lobe, (D) the insula, and (E) right temporo-parieto-occipital junction. Within the cortical regions where most CMBs occurred, the average shortest distance between the cortex and the nearest CMB was $\mu \pm \sigma = 7.1 \pm 1.8$ mm.

Analysis 1

MANOVA identified WM structures whose mean FAs were significantly associated with sex, age, and CMB counts (Table 1, Figs. 2, 3, and 4). For the acute timepoint, Table 1 shows a multivariate main effect of age on the GCC ($F_{2,104} = 19.85$, $p < 0.001$, $\eta^2 = 0.28$), BCC ($F_{2,104} = 9.07$, $p < 0.001$, $\eta^2 = 0.21$), and SCC ($F_{2,104} = 4.03$, $p = 0.021$, $\eta^2 = 0.07$), on the ILFs ($F_{2,104} = 4.20$, $p = 0.02$, $\eta^2 = 0.07$), MdLFs ($F_{2,104} = 4.25$, $p = 0.017$, $\eta^2 = 0.08$), Sup-F fasciculi ($F_{2,104} = 8.09$, $p = 0.001$, $\eta^2 = 0.14$), and Sup-T fasciculi ($F_{2,104} = 13.70$, $p < 0.001$, $\eta^2 = 0.21$). Table 1 also indicates a multivariate main effect of sex on

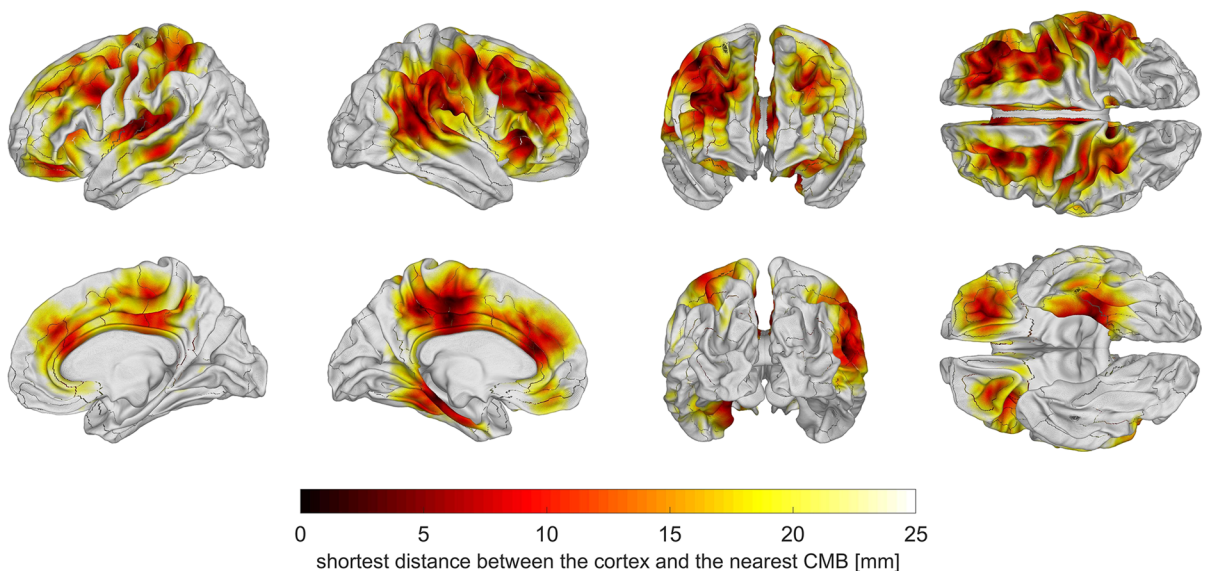


Fig. 1 Cortical map of average shortest distances from the GM/WM interface to the nearest CMB. To generate this map, the distance between each cortical mesh vertex and the closest CMB was calculated for each subject, and this distance was plotted on the cortical surface. The subjects' cortical maps were transformed to a common average template (atlas) and averaged over to generate the map above. CMBs were local-

ized near the cortical surface within the lateral and medial aspects of the frontal and parietal lobes, orbitofrontal cortex, the temporal lobes, the insulae, and the right temporo-parieto-occipital junction. Within these cortical regions, the average shortest distance between the cortex and the nearest CMB was $\mu \pm \sigma = 7.1 \pm 1.8$ mm

Table 1 Results of the multivariate analysis of variance (MANOVA, statistical analysis 1)

Structure	Timepoint	Variable	$F_{2, 104}$	p	η^2	Power
GCC	Acute	Age	19.85	0.001	0.28	1.00
		Sex	0.04	0.958	0.00	0.06
		CMBs	0.87	0.423	0.02	0.20
	Chronic	Age	22.70	0.001	0.30	1.00
		Sex	0.21	0.808	0.00	0.08
		CMBs	0.21	0.812	0.00	0.08
BCC	Acute	Age	9.07	0.001	0.21	1.00
		Sex	0.62	0.604	0.02	0.18
		CMBs	0.85	0.468	0.02	0.23
	Chronic	Age	6.82	0.001	0.17	0.97
		Sex	1.81	0.150	0.05	0.46
		CMBs	0.03	0.993	0.00	0.05
SCC	Acute	Age	4.03	0.021	0.07	0.71
		Sex	0.87	0.424	0.02	0.20
		CMBs	1.08	0.342	0.02	0.24
	Chronic	Age	0.40	0.671	0.01	0.11
		Sex	0.54	0.585	0.01	0.14
		CMBs	0.38	0.688	0.01	0.11
ILF	Acute	Age	4.20	0.020	0.08	0.73
		Sex	1.85	0.162	0.03	0.38
		CMBs	1.04	0.259	0.02	0.23
	Chronic	Age	3.26	0.042	0.06	0.61
		Sex	0.32	0.725	0.01	0.10
		CMBs	0.72	0.425	0.06	0.61
MdLF	Acute	Age	4.25	0.017	0.08	0.73
		Sex	2.34	0.102	0.04	0.46
		CMBs	0.54	0.587	0.01	0.14
	Chronic	Age	3.20	0.045	0.06	0.60
		Sex	1.00	0.371	0.02	0.22
		CMBs	2.73	0.070	0.05	0.53
IOFF	Acute	Age	0.43	0.653	0.01	0.12
		Sex	1.26	0.287	0.02	0.27
		CMBs	1.44	0.242	0.03	0.30
	Chronic	Age	0.12	0.886	0.00	0.07
		Sex	5.59	0.005	0.10	0.85
		CMBs	1.14	0.249	0.03	0.30
Sup-F	Acute	Age	8.09	0.001	0.14	0.95
		Sex	1.19	0.309	0.02	0.26
		CMBs	0.44	0.643	0.01	0.12
	Chronic	Age	5.64	0.005	0.10	0.85
		Sex	1.28	0.283	0.02	0.27
		CMBs	0.14	0.879	0.00	0.07

Table 1 (continued)

Structure	Timepoint	Variable	$F_{2, 104}$	p	η^2	Power
Sup-T	Acute	Age	8.76	0.001	0.14	0.97
		Sex	3.26	0.042	0.06	0.61
		CMBs	0.12	0.886	0.00	0.07
	Chronic	Age	13.70	0.001	0.21	1.00
		Sex	0.32	0.729	0.01	0.10
		CMBs	0.45	0.641	0.01	0.12

The mean FAs of the left and right WM structures of interest were included as one bivariate vector of dependent variables. Participants' ages, sex, and CMB counts were independent variables. Acute and chronic data were acquired ~ 7 days and ~ 6 months post-injury, respectively. Null hypotheses were tested at a significance level of $\alpha = 0.05$, and significant findings are in **bold case**. F statistics with 2 and 104 degrees of freedom, effect sizes (Cohen's η^2), and statistical power are listed

BCC, body of the corpus callosum; *CMB*, cerebral microbleed; *CST*, corticospinal tract; *FA*, fractional anisotropy; *GCC*, genu of the corpus callosum; *ILF*, inferior longitudinal fasciculus; *IOFF*, inferior occipitofrontal fasciculus; *MdLF*, middle longitudinal fasciculus; *SCC*, splenium of the corpus callosum; *Sup-F*, superficial frontal; *Sup-P*, superficial parietal; *Sup-T*, superficial temporal; *WM*, white matter

Sup-T fasciculi ($F_{2, 104} = 3.26$, $p = 0.042$, $\eta^2 = 0.06$) at the acute timepoint. For the chronic timepoint, Table 1 indicates a multivariate main effect of age on the GCC ($F_{2, 104} = 22.70$, $p < 0.001$, $\eta^2 = 0.30$) and BCC ($F_{2, 104} = 6.82$, $p < 0.001$, $\eta^2 = 0.17$), on the ILFs ($F_{2, 104} = 3.26$, $p = 0.042$, $\eta^2 = 0.06$), MdLFs ($F_{2, 104} = 3.20$, $p = 0.045$, $\eta^2 = 0.06$), Sup-F fasciculi ($F_{2, 104} = 5.64$, $p = 0.005$, $\eta^2 = 0.10$), and Sup-T fasciculi ($F_{2, 104} = 13.70$, $p < 0.001$, $\eta^2 = 0.21$). Table 1 also reports a multivariate main effect of sex on the IOFFs ($F_{2, 104} = 5.59$, $p = 0.001$, $\eta^2 = 0.14$) for the chronic timepoint. CMB counts had no significant effects on mean FAs at either timepoint.

Analysis 2

Repeated-measures MANOVA identified significant mean FA changes (Table 2, Figs. 1, 2, 3, and 4) within the anterior BCC (Hotelling's $T_{108}^2 = 3.04$, $p = 0.003$, Cohen's $d = 0.29$), posterior BCC ($T_{108}^2 = 2.68$, $p = 0.009$, $d = 0.26$) and SCC ($T_{108}^2 = 2.47$, $p = 0.015$, $d = 0.24$), the left Sup-F fasciculi ($T_{108}^2 = 2.72$, $p = 0.008$, $d = 0.26$), and the left branch of the CST ($T_{108}^2 = 2.77$, $p = 0.007$, $d = 0.27$). CMB counts had no significant effects on mean FA changes. WM fasciculi with significant findings are displayed together for simultaneous illustration in Fig. 5.

Analysis 3

Factorial MANOVA revealed the significant individual contributions of age, sex, or CMB count to mean FA changes (Table 3) above and beyond those of other contributions. For the acute timepoint, there was a multivariate main effect of age on the BCC ($F_{45, 11} = 2.61$, $p = 0.04$, $\eta^2 = 0.91$), but no significant interactions. For the chronic timepoint, there was a multivariate main effect of age on the GCC ($F_{46, 11} = 5.52$, $p < 0.001$, $\eta^2 = 0.96$), BCC ($F_{46, 11} = 3.99$, $p = 0.01$, $\eta^2 = 0.94$), and MdLFs ($F_{46, 11} = 2.61$, $p = 0.04$, $\eta^2 = 0.92$). There was also a multivariate main effect of CMB count on the BCC ($F_{7, 11} = 3.33$, $p = 0.04$, $\eta^2 = 0.68$) and MdLFs ($F_{7, 11} = 3.34$, $p = 0.04$, $\eta^2 = 0.68$). We identified a significant age-by-sex interaction on the GCC ($F_{6, 11} = 3.92$, $p = 0.02$, $\eta^2 = 0.68$) and a significant age-by-CMB-count interaction on the GCC ($F_{21, 11} = 3.02$, $p = 0.03$, $\eta^2 = 0.85$).

Discussion

Aside from statistical analyses, our study provides convenient visualizations of the strongest spatiotemporal associations between WM fasciculi and effects

Fig. 2 WM fasciculi whose mean FAs are significantly associated with age at injury either acutely or chronically. Fiber trajectories are encoded by colors (red: left–right; green: anterior–posterior; blue: inferior–superior). Axial, sagittal, and coronal views of WM structures are superimposed on a translucent model of the brain. The gyri and sulci connected by the corresponding WM pathways are also displayed. **(A)** GCC damage is associated with deficits of functions localized to the frontal and prefrontal cortex, including executive function and interhemispheric communication [24]. **(B)** BCC damage is frequently associated with somatomotor deficits [26]. **(C)** SCC injury can result in damage to circuits mediating visual, auditory, and somatosensory function, as well as multimodal sensory integration [25]

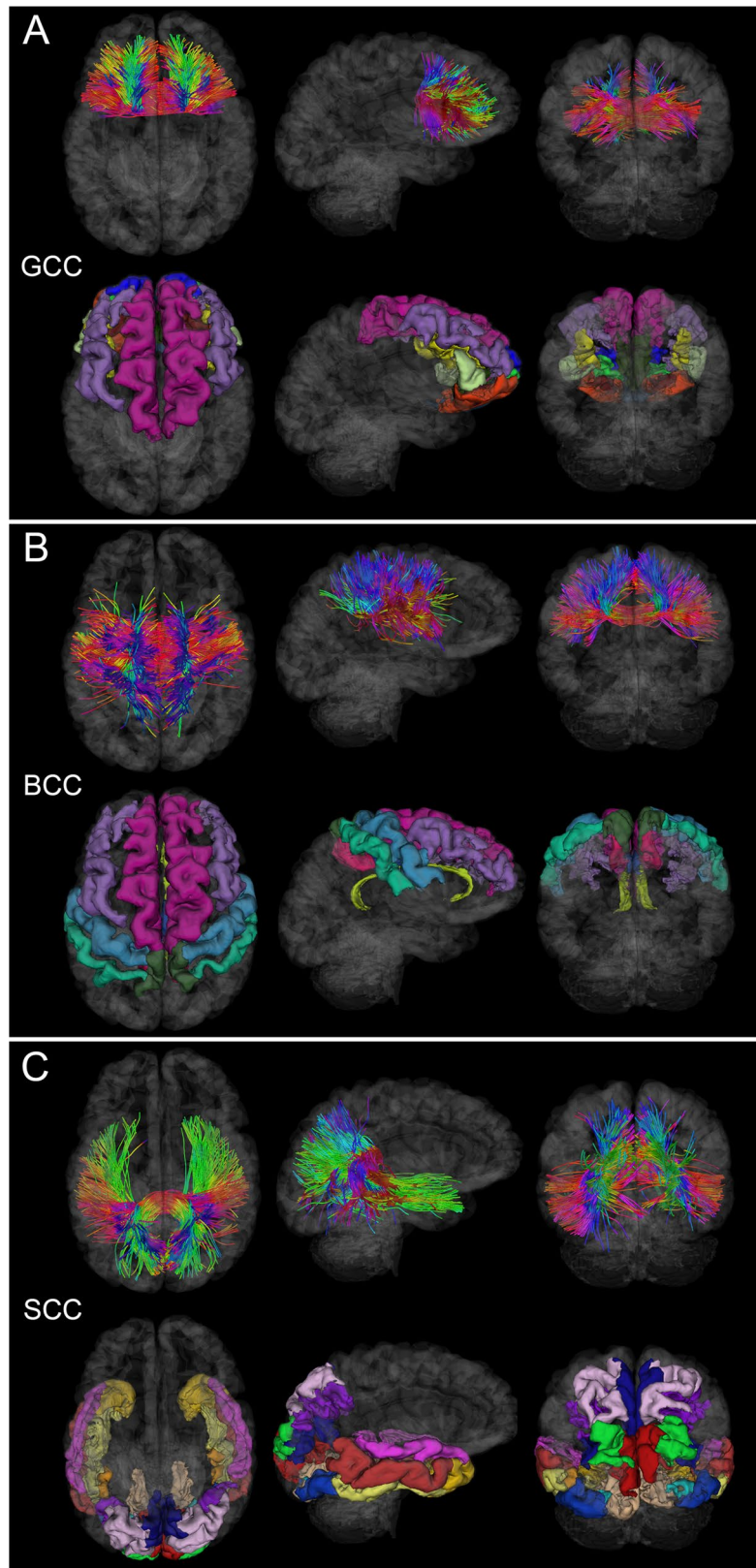


Fig. 3 Like Fig. 2, for the MdLF, ILF, and IOFF. (A) MdLF damage can result in deficits of attention [31] and both visual and auditory information processing [30]. (B) ILF injury may be associated with deficits in the processing of complex information associated with visual object recognition [35]. (C) IOFF degradation may result in damage to visual and motor pathways [35]

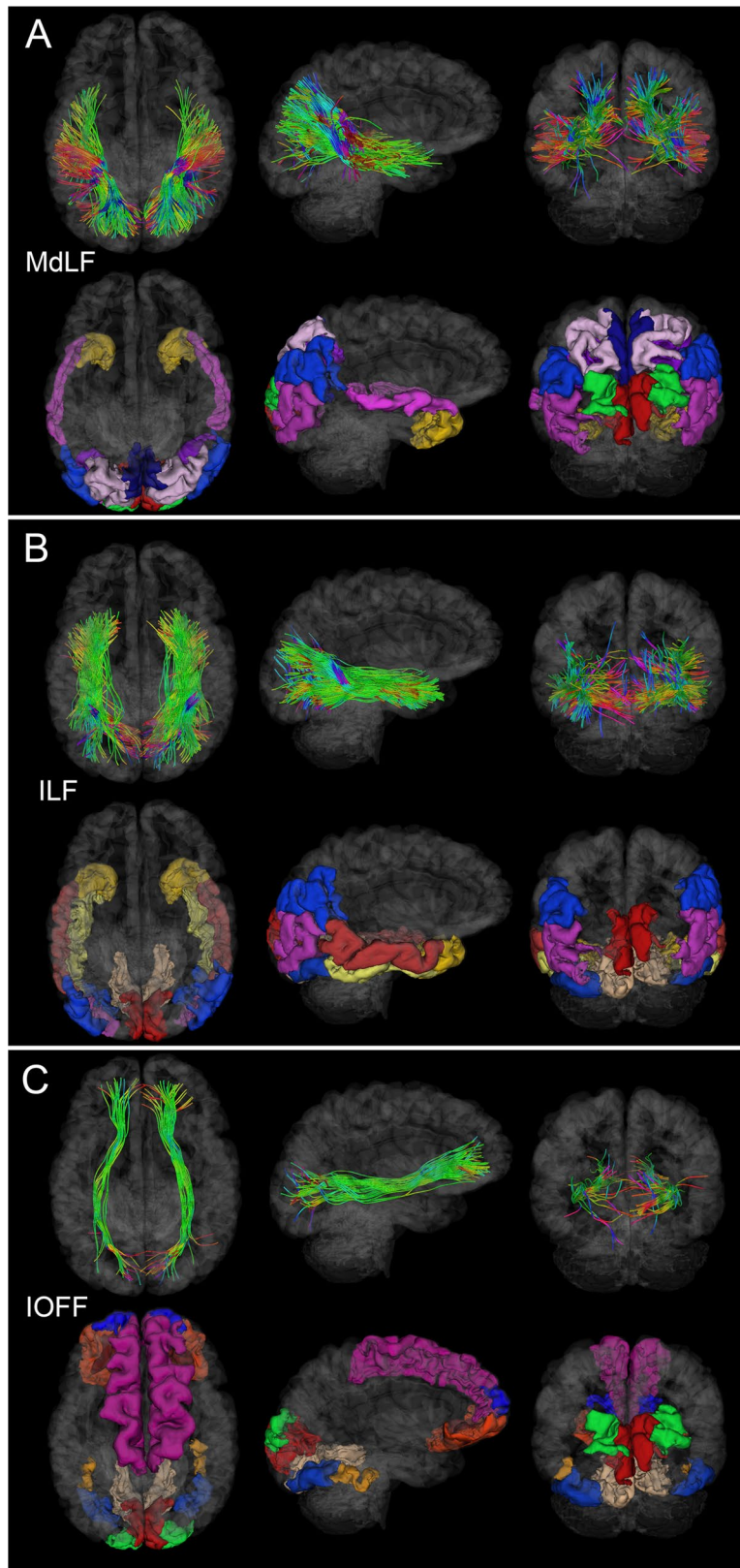


Table 2 Results of paired-sample *t*-tests for the null hypothesis of no change in mean FA between the acute and chronic time points (statistical analysis 2)

Structure	μ	σ	95% CI	T^2_{108}	<i>p</i>	<i>d</i>
Anterior GCC	0.00	0.77	[-0.14, 0.15]	0.00	0.998	0.00
Posterior GCC	0.04	0.60	[-0.07, 0.16]	0.75	0.458	0.07
Anterior BCC	0.06	0.63	[-0.06, 0.18]	1.04	0.302	0.10
Middle BCC	0.20	0.68	[-0.07, 0.33]	3.04	0.003	0.29
Posterior BCC	0.20	0.79	[-0.05, 0.35]	2.68	0.009	0.26
Anterior SCC	0.04	0.75	[-0.10, 0.18]	0.55	0.587	0.05
Posterior SCC	0.19	0.81	[-0.04, 0.35]	2.47	0.015	0.24
Left ILF	0.04	0.57	[-0.07, 0.14]	0.64	0.524	0.06
Right ILF	0.04	0.72	[-0.10, 0.17]	0.54	0.587	0.05
Left MdLF	0.06	0.84	[-0.10, 0.22]	0.76	0.452	0.07
Right MdLF	0.13	0.72	[-0.01, 0.26]	1.90	0.063	0.18
Left Sup-F	0.17	0.67	[-0.05, 0.20]	2.72	0.008	0.26
Right Sup-F	0.08	0.66	[-0.04, 0.21]	1.30	0.197	0.12
Left Sup-T	0.04	0.96	[-0.14, 0.23]	0.46	0.643	0.04
Right Sup-T	0.11	0.96	[-0.08, 0.29]	1.16	0.247	0.11
Left Sup-P	0.11	0.73	[-0.03, 0.24]	1.53	0.129	0.15
Right Sup-P	0.08	0.64	[-0.04, 0.20]	1.32	0.190	0.13
Left IOFF	0.01	0.79	[-0.14, 0.16]	0.11	0.913	0.01
Right IOFF	0.12	0.77	[-0.03, 0.27]	1.60	0.113	0.15
Left CST	0.22	0.84	[-0.06, 0.38]	2.77	0.007	0.27
Right CST	0.09	0.88	[-0.07, 0.26]	1.11	0.268	0.11

The mean μ and standard deviation σ of the time difference in mean standardized residuals for mean FA are listed. The null hypothesis was tested at a significance level of $\alpha = 0.05$, and significant findings are displayed in **bold case**. Hotelling's T^2 statistics with 108 degrees of freedom, effect sizes (Cohen's *d*), and statistical power are listed

BCC, body of the corpus callosum; *CST*, corticospinal tract; *GCC*, genu of the corpus callosum; *ILF*, inferior longitudinal fasciculus; *IOFF*, inferior occipitofrontal fasciculus; *MdLF*, middle longitudinal fasciculus; *SCC*, splenium of the corpus callosum; *Sup-F*, superficial frontal; *Sup-P*, superficial parietal; *Sup-T*, superficial temporal

due to age, sex, and time (Fig. 5). In what follows, we discuss these and related findings as they pertain to effects associated with age, sex, CMBs, biomechanics, demyelination, and natural aging.

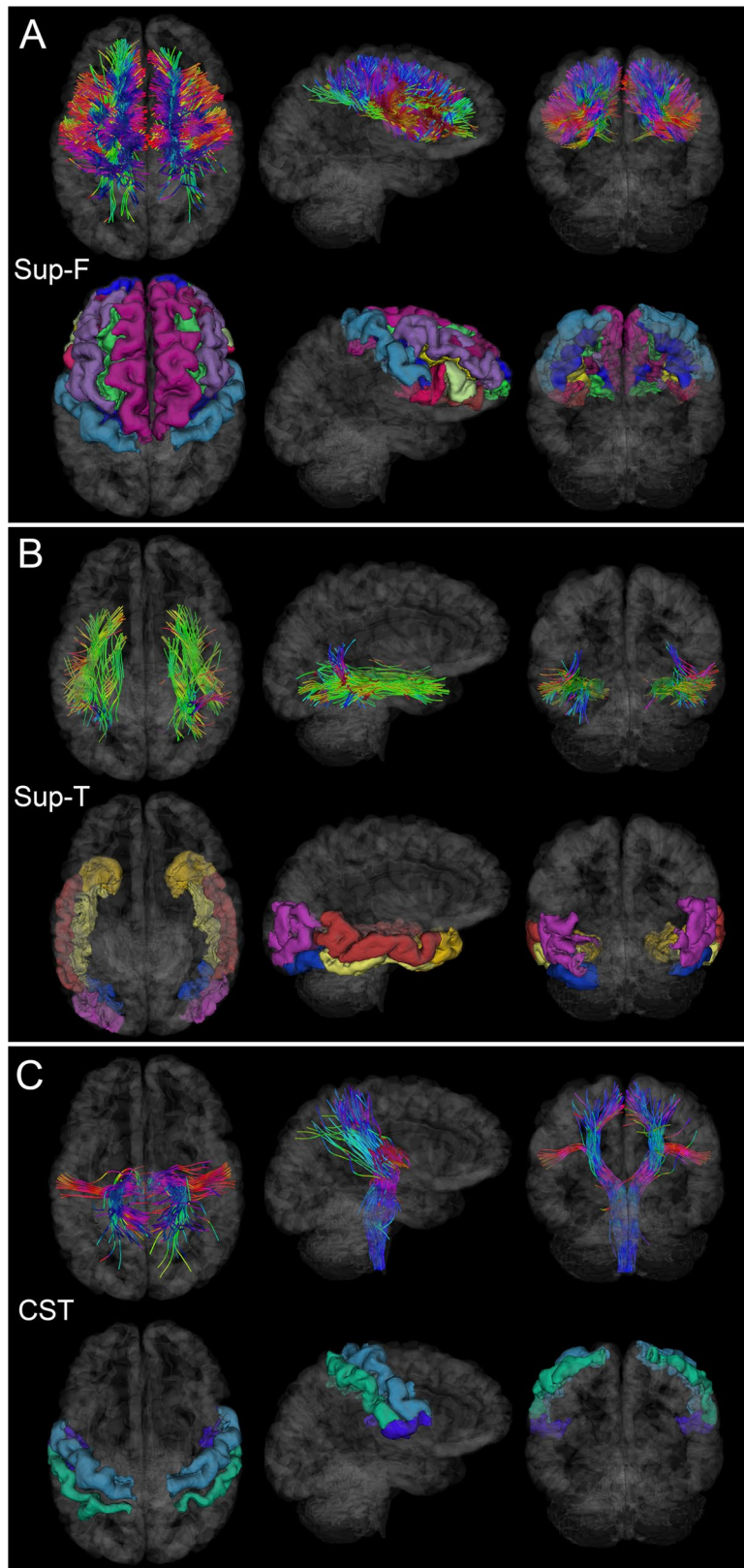
Age effects

Whereas the literature on age-related effects in *moderate-to-severe* TBI is extensive, studies like ours on how age at injury modulates *mild* TBI sequelae remain scarce. Nevertheless, extensive research supports our findings on the progressive effects of age at injury on TBI-related WM degradation and on subsequent cognitive and functional impairments [15–20, 21, 22, 23]. Below, we describe age-related WM

alterations after mTBI and postulate their potential associations with cognitive and functional impairment based on this existing body of knowledge.

Our results suggest that age at injury has a linear association with CC degradation (Table 1), likely due not only to TBI, but also to the accumulative effect of other pathologies and to their interactions with TBI. The associations between mean FA decrease in the GCC and BCC and this variable are significant. Furthermore, age at injury is associated with significantly lower mean FA in the SCC at the acute—but not chronic—timepoint. WM degradation observed both acutely and chronically in the GCC could be associated with motor coordination decline [24], such that our findings may underscore how injuries to this WM structure can translate into neurological deficits

Fig. 4 Like Fig. 2, for the Sup-F, Sup-T, and CST. (A) Sup-F fasciculi affected by injury can result in deficits of executive control [28]. (B) Sup-T fasciculi, when affected significantly by injury, may result in deficits pertaining to the recognition of faces and objects. (C) CST damage can affect the functions of the primary somatomotor cortex [40]



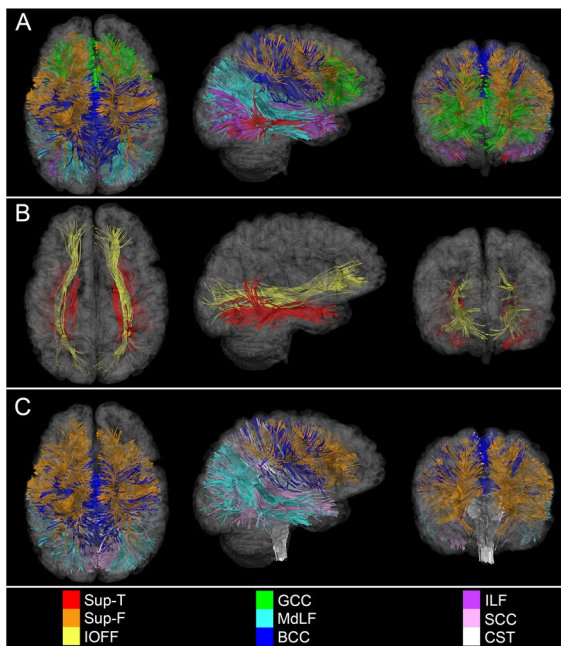


Fig. 5 Simultaneous visualization of WM structures with the most significant statistical associations. Displayed are WM fasciculi with the most statistically significant associations between mean FA, on the one hand, and (A) age, (B) sex, as well as (C) time, on the other hand. These depictions emphasize the potential WM degradation substrates of post-traumatic executive dysfunction (as reflected in the vulnerability of Sup-F fasciculi to injury), audiovisual impairment and attention deficits (highlighted by WM degradation within the MdLF), and motor deficits (underlined by degeneration of the CST). Axial, sagittal, and coronal views of each WM structure are superimposed on translucent models of the GM surface

whose typical severity increases with age. Older adults' significantly lower mean FA in the GCC and SCC have been associated with declines in reading speed and comprehension [25], two cognitive abilities that rely on the speed of interhemispheric information transfer, a key CC function. Funnell et al. [26] found that the anterior midbody of the CC transmits motor information, whereas the posterior midbody transmits somatosensory information between hemispheres. Ota et al. [27] showed that age at injury is correlated with the FAs of the GCC and anterior BCC. Thus, our results indicate that mTBI may accelerate aging-related WM FA decrease in the CC and could contribute to a faster decline of motor functioning, processing speed, and interhemispheric information transfer.

Whereas superficial WM tracts are challenging to investigate due to their structural complexity and

inter-subject variability, our study benefits from an approach with validated high consistency in mapping such tracts. Aside from the CC, Sup-F and Sup-T fasciculi also exhibit mean FA decreases whose magnitudes increase with age (Table 1). Sup-F fasciculi consist of relatively short-range connections between ipsilateral frontal areas, whereas Sup-T fasciculi connect GM regions within temporal lobes (Fig. 4). In agreement with our findings of reduced mean FA within superficial WM, a study of youths aged 8–22 by Stojanovski et al. [28] concluded that mTBI damage can lead to FA decreases within superficial WM and to connectivity damage typically associated with deficits of attention and processing speed. Our findings complement these and suggest that WM integrity reductions in the superficial WM of pediatric TBI patients are similar to those observed in adulthood. Future studies should explore if these structural findings translate into attention and processing speed deficits.

The evidence on the existence of a spatial gradient in age-related superficial WM reductions is equivocal. Phillips et al. [29] found an anteroposterior gradient of age-related FA reductions in superficial frontal WM which, they suggested, is more vulnerable to aging effects than that in occipital areas. By contrast, Table 1 and Fig. 4 suggest that, relative to anterior Sup-F fasciculi ($\eta^2 = 0.10$), posterior Sup-T fasciculi experience larger mean FA decreases with age ($\eta^2 = 0.21$). Thus, more research on the existence of an anteroposterior gradient in age-related superficial WM changes is needed.

Compared to younger participants, older adults exhibited lower mean FAs in the MdLFs and ILFs, both acutely and chronically (Table 1). The MdLF is a major pathway in the dorsal stream of semantic processing, with roles in language comprehension, visuospatial integration, attentional processing, and audiovisual integration. Herbert et al. [30] describe the ILF as a significant component of the semantic ventral stream and indicate that structural IF alterations are associated with semantic/lexical retrieval impairments and visual agnosia. Goldstein and Levin [31] highlight that older adults' effortful attention and language processing (i.e., visual naming and word association) are significantly impaired after mTBI. Thus, the relationship found here between older age and larger mean FA decreases in the MdLFs and ILFs

Table 3 Results of MANOVA investigating whether each predictor (age, sex, or CMB count) contributed significantly, above and beyond the contributions of all other predictors, to the changes in FA means observed in various structures (statistical analysis 3)

Structure	Stage	Variable(s)	<i>F</i>	<i>df</i> ₁	<i>df</i> ₂	<i>p</i>	η^2	Power
GCC	Acute	CMB	1.20	7	11	0.38	0.43	0.31
		Age	1.82	45	11	0.14	0.88	0.64
		Sex	0.67	2	10	0.54	0.12	0.13
		Sex × age	0.64	6	11	0.70	0.26	0.17
		CMBs × age	1.38	22	11	0.30	0.73	0.45
	Chronic	CMB	0.73	7	11	0.65	0.32	0.19
		Age	5.52	46	11	0.01	0.96	1.00
		Sex	0.16	2	10	0.86	0.03	0.07
		Sex × age	3.92	6	11	0.02	0.68	0.81
		CMB × age	3.02	21	11	0.03	0.85	0.85
BCC	Acute	CMB	1.14	7	11	0.41	0.42	0.29
		Age	2.61	45	11	0.04	0.91	0.83
		Sex	0.01	3	9	1.00	0.00	0.05
		Sex × age	1.85	6	11	0.18	0.50	0.45
		CMB × age	1.00	22	11	0.53	0.67	0.33
	Chronic	CMB	3.33	7	11	0.04	0.68	0.76
		Age	3.99	46	11	0.01	0.94	0.96
		Sex	1.04	3	9	0.42	0.26	0.20
		Sex × age	1.68	6	11	0.22	0.48	0.41
		CMB × age	1.89	21	11	0.14	0.78	0.61
SCC	Acute	CMB	0.61	7	11	0.74	0.28	0.17
		Age	1.34	45	11	0.31	0.85	0.48
		Sex	0.03	2	10	0.97	0.01	0.05
		Sex × age	0.46	6	11	0.82	0.20	0.13
		CMB × age	0.61	22	11	0.85	0.55	0.20
	Chronic	CMB	1.14	7	11	0.41	0.42	0.29
		Age	2.33	46	11	0.06	0.91	0.78
		Sex	1.20	2	10	0.34	0.19	0.21
		Sex × age	1.37	6	11	0.31	0.43	0.34
		CMB × age	1.79	21	11	0.16	0.77	0.58
ILF	Acute	CMB	1.82	7	11	0.18	0.54	0.46
		Age	2.49	45	11	0.05	0.91	0.81
		Sex	0.24	2	10	0.79	0.05	0.08
		Sex × age	1.11	6	11	0.42	0.38	0.27
		CMB × age	1.91	22	11	0.13	0.79	0.62
	Chronic	CMB	2.75	7	11	0.07	0.64	0.66
		Age	1.03	46	11	0.52	0.81	0.37
		Sex	0.46	2	10	0.64	0.08	0.11
		Sex × age	2.16	6	11	0.13	0.54	0.52
		CMB × age	1.21	21	11	0.39	0.70	0.39

could underlie post-traumatic deficits in attention and language processing.

Within both the CC and superficial cerebral fasciculi, WM degradation occurs with typical aging. We found the GCC to be more susceptible to degradation than the SCC, both acutely and chronically

(Table 2). However, because this effect has also been documented in normal aging, it is possible that TBI only accelerates post-traumatic CC degradation already underway due to aging. Similarly, the mean FA of superficial WM tracts was found to decrease with both age and injury chronicity (Tables 1 and 2).

Table 3 (continued)

Structure	Stage	Variable(s)	<i>F</i>	<i>df</i> ₁	<i>df</i> ₂	<i>p</i>	η^2	Power
MdLF	Acute	CMB	1.53	7	11	0.25	0.49	0.39
		Age	1.20	45	11	0.39	0.83	0.43
		Sex	1.15	2	10	0.35	0.19	0.20
		Sex × age	0.89	6	11	0.53	0.33	0.22
		CMB × age	1.24	7	11	0.37	0.71	0.41
	Chronic	CMB	3.34	45	11	0.04	0.68	0.76
		Age	2.61	2	10	0.04	0.92	0.83
		Sex	0.85	6	11	0.45	0.15	0.16
		Sex × age	0.85	22	11	0.56	0.32	0.21
		CMB × age	1.51	7	11	0.24	0.74	0.49
IOFF	Acute	CMB	0.52	46	11	0.81	0.25	0.15
		Age	1.09	45	11	0.47	0.82	0.39
		Sex	1.11	2	10	0.37	0.18	0.19
		Sex × age	1.11	6	11	0.42	0.38	0.27
		CMB × age	1.17	22	11	0.41	0.70	0.38
	Chronic	CMB	0.71	7	11	0.66	0.31	0.19
		Age	1.06	46	11	0.49	0.82	0.38
		Sex	1.46	2	10	0.28	0.23	0.24
		Sex × age	0.83	6	11	0.57	0.31	0.21
		CMB × age	1.16	21	11	0.41	0.69	0.38
Sup-F	Acute	CMB	1.35	7	11	0.31	0.46	0.35
		Age	1.59	45	11	0.21	0.87	0.57
		Sex	0.31	2	10	0.74	0.06	0.09
		Sex × age	1.23	6	11	0.36	0.40	0.30
		CMB × age	2.15	22	11	0.09	0.81	0.68
	Chronic	CMB	2.55	7	11	0.08	0.62	0.62
		Age	2.50	46	11	0.05	0.91	0.81
		Sex	1.83	2	10	0.21	0.27	0.29
		Sex × age	2.74	6	11	0.07	0.60	0.63
		CMB × age	1.79	21	11	0.16	0.77	0.58
Sup-T	Acute	CMB	1.10	7	11	0.43	0.41	0.28
		Age	1.90	45	11	0.12	0.89	0.67
		Sex	1.99	2	10	0.19	0.29	0.32
		Sex × age	1.10	6	11	0.42	0.38	0.27
		CMB × age	1.36	22	11	0.30	0.73	0.45
	Chronic	CMB	3.69	7	11	0.03	0.70	0.81
		Age	2.42	46	11	0.06	0.91	0.79
		Sex	0.54	2	10	0.60	0.10	0.12
		Sex × age	1.86	6	11	0.18	0.50	0.45
		CMB × age	2.10	21	11	0.10	0.80	0.66

Table 3 (continued)

Structure	Stage	Variable(s)	<i>F</i>	<i>df</i> ₁	<i>df</i> ₂	<i>p</i>	η^2	Power
Sup-P	Acute	CMB	2.86	7	11	0.06	0.65	0.68
		Age	1.62	45	11	0.19	0.87	0.58
		Sex	0.27	2	10	0.77	0.05	0.08
		Sex × age	1.68	6	11	0.22	0.48	0.41
		CMB × age	0.90	22	11	0.60	0.64	0.29
	Chronic	CMB	1.05	7	11	0.45	0.40	0.27
		Age	1.11	46	11	0.46	0.82	0.40
		Sex	0.16	2	10	0.85	0.03	0.07
		Sex × age	2.02	6	11	0.15	0.52	0.49
		CMB × age	0.96	21	11	0.56	0.65	0.31
CST	Acute	CMB	1.14	7	11	0.41	0.42	0.29
		Age	1.53	45	11	0.23	0.86	0.55
		Sex	1.16	2	10	0.35	0.19	0.20
		Sex × age	0.72	6	11	0.65	0.28	0.18
		CMB × age	1.10	22	11	0.46	0.69	0.36
	Chronic	CMB	1.20	7	11	0.38	0.43	0.31
		Age	1.01	46	11	0.53	0.81	0.36
		Sex	0.69	2	10	0.52	0.12	0.14
		Sex × age	1.19	6	11	0.38	0.39	0.29
		CMB × age	1.62	21	11	0.21	0.76	0.53

The acute and chronic time points correspond to ~7 days and ~6 months post-injury, respectively. Null hypotheses were tested at a significance level of $\alpha = 0.05$, and findings that are both significant and well-powered (power > 0.8) are in **bold case**. *F* statistics, numerator and denominator degrees of freedom (*df*₁ and *df*₂), effect sizes (Cohen's η^2), and statistical power are listed.

BCC, body of the corpus callosum; CMB, cerebral microbleed; CST, corticospinal tract; FA, fractional anisotropy; GCC, genu of the corpus callosum; ILF, inferior longitudinal fasciculus; IOFF, inferior occipitofrontal fasciculus; MdLF, middle longitudinal fasciculus; SCC, splenium of the corpus callosum; Sup-F, superficial frontal; Sup-P, superficial parietal; Sup-T, superficial temporal; WM, white matter

However, FA decreases in *superficial* WM are more strongly associated with age-related cognitive decline than those in *deep* WM [32], which suggests the hypothesis that the former are more strongly associated with cognitive decline than the latter. Tables 1 and 2 suggest that the degradation of superficial WM in frontal and temporal lobes depends significantly on injury chronicity and age at injury. Because changes in executive function, personality, and memory are strongly mediated by superficial neural circuits in frontal and temporal areas, future research should seek to deepen our insights on the interaction between TBI and age-related cognitive decline in these regions, which are highly vulnerable to injury.

Importantly, falls in older adults can be secondary to vascular brain injury or to neurodegenerative diseases like Parkinson's disease, Lewy body dementia,

and normal-pressure hydrocephalus. Although our study participants did not have documented histories of such conditions, they were not specifically screened for them either. Because such diseases can alter WM integrity above and beyond TBI alone, some of our findings may be partially due to such (undiagnosed) neurological disorders; we acknowledge this as a weakness of our study.

Sex effects

Consistently, males have been found to be relatively more vulnerable to WM degradation post-TBI [33]. For example, male sex predicts lower mean FA values in Sup-T fasciculi (Fig. 4). In agreement with our findings, Fakhra et al. [34] found a similar male sex-related vulnerability to WM degradation and to

cognitive impairment after TBI. However, in contrast to our study, these authors found significant sex-related differences in WM degradation only in the uncinate fasciculus (UF). Although our analysis did not isolate the UF, Sup-T fasciculi are adjacent to it. Thus, the discrepancy between our study and that of Fakhran et al. may be due to methodological differences, at least pertaining to tractography. Nevertheless, because the integrity of superficial WM is a biomarker of age-related cognitive decline [32], males' lower FA in Sup-T fasciculi compared to females' (Table 1) could partly explain males' more appreciable impairment of functions modulated by these circuits.

Table 1 indicates a significant relationship between male sex and lower mean FA in the IFOFs after TBI. The IFOF is a direct ventral route for the semantic network involved in language processing, object use, and object recognition. In agreement with our findings, another study [35] found that reduced post-traumatic IFOF integrity are associated with (non) verbal semantic task performance deficits. Thus, IFOF involvement in semantic processing suggests that lower mean FA values in males' IFOFs could be associated with more severe impairments of semantic processing networks.

CMB effects

CMBs are relatively more common in older adults and, in a post-traumatic setting, SWIs can reveal both traumatic and non-traumatic CMBs. For example, some non-traumatic CMBs can be linked to vascular or metabolic disease, and to risk factors like hypercholesterolemia and hypertension. Because CMB etiology could not be ascertained, it is possible that at least some CMB identified here were non-traumatic. Thus, the CMB-related effects discussed here in the context of post-traumatic WM degradation may not be related to TBI alone. For this reason, our post-traumatic CMB findings should be interpreted with caution. Specifically, although our results indicate that CMB findings are a risk factor for post-traumatic WM degradation, that risk is not necessarily TBI-related. Future studies should establish the distinct contributions of traumatic vs. non-traumatic CMBs to post-traumatic WM degradation.

CMB count has been identified as an injury severity marker and is linked to increased risk for cognitive

impairment [36, 37]. Our findings complement those of previous studies and suggest that the relationship between CMBs identified after TBI and WM degradation could help to prognosticate the risk of chronic cognitive deficits. Lawrence et al. [36] found a significant association between GCS and post-traumatic CMB count. They suggest that acute CMB identification could aid to improve the accuracy of TBI severity estimation. In our study, the mean FAs of the BCC, MdLF, and Sup-T fasciculi are significantly and negatively associated with CMB count (Table 3), which highlights the putative relationship between CMB count and WM degradation. Our analysis does not account for CMBs' anatomical locations, which could moderate the extent of TBI-related cognitive decline. For this reason, future studies should investigate how CMB locations impact WM.

Biomechanical effects

This study illustrates how TBI biomechanics translate into WM degradation patterns. For example, we document significant mean FA decreases within the commissural tracts (BCC and SCC), right MdLF, left Sup-F tracts, and left CST (Table 1). Callosal WM is relatively more vulnerable to post-traumatic degradation for two primary reasons. Firstly, its connections are interhemispheric, which renders them more vulnerable to traumatic forces and to mechanical strain [38]. Secondly, the CC is relatively less myelinated than other WM structures, which makes it more fragile. Thirdly, because the CC connects the brain hemispheres, this structure plays a key role in conferring mechanical stability and integrity to the telencephalon. Since the hemispheres are relatively large and mechanically inert, the physical momenta of TBI forces can be easily transferred biomechanically to the CC, where they can lead to shearing, twisting, and tearing commissural axons.

Bigler et al. [39] found that TBI of the temporal stem (TS), as inferred using diffusion tensor imaging, correlates with specific FA decreases in the ILF, arcuate fasciculus, and IFOF, as well as with memory impairments modulated by injuries to these structures. Because our findings indicate post-traumatic FA decreases in the ILF, arcuate fasciculus and IFOF, the findings of Bigler et al. provide context to our own. Conta and Stelzner [40] showed that CST axons are much more vulnerable to injury than other

supraspinal projections, partly because TBI is often associated with sudden forces imparted to the neck and brainstem. CST axons are exceptionally long (since they extend along the brain stem and spinal cord), such that mechanical forces can affect them more than they impact the relatively shorter WM tracts encased within—and protected by—the cranial cavity.

Demyelination effects

The MdLF, a prominent cerebral association fiber tract, runs principally between the superior temporal gyrus and the parietal lobe [41, 42]. The extent of demyelination along this WM structure has been related to impairments in the ability to distinguish tone pitch and to process speech sounds [43]. Relatedly, the TS is a major WM structure that bridges the temporal and frontal lobes and that includes fibers traversing temporal WM, such as the ILF, UF, and IFOF. The myelination of superficial WM axons terminates last during brain development (i.e., as late as the fourth and fifth decades of life), which may partly explain the relatively high vulnerability of superficial axons to blunt trauma during ongoing myelination [44]. Furthermore, oligodendrocytes in superficial WM provide less myelination to axons compared to those in deep WM, thus offering less protection to superficial WM and conferring to it a higher vulnerability to axonal damage [45]. These findings may explain our own results, which indicate that superficial WM is affected significantly by mTBI. The fact that frontotemporal injuries are among the most common types of TBI further highlights the high susceptibility of superficial frontal and temporal WM to trauma. Because post-traumatic degradation of superficial WM has not been quantified systematically, our findings are illustrative of typical frontotemporal TBI effects even in *mild* TBI, where the WM at highest injury risk includes superficial dorsolateral WM in frontal, temporal, parietal, and occipital areas. This, in conjunction with the fact that ~75 to 90% of all TBIs are mild, highlights the potential significance of our findings, and the importance of quantifying superficial WM degradation.

Natural aging effects

Our study compares only the acute and chronic (~7 days and ~6 months post-injury, respectively)

stages of mTBI. However, Edlow et al. [46] suggest that quantifiers of the *sub-acute* stage of an injury (~8 days to rehabilitation discharge) may better predict functional outcomes than measures obtained during the acute stage. Thus, to further understand the roles of age, sex, and CMBs on WM degradation, future studies should monitor TBI patients sub-acute and across longer time intervals, including ~1 year post-injury and beyond. Due to limitations related to data availability and statistical power, this cohort study does not include healthy controls (HCs). For this reason, we could not directly quantify the relative extent to which the structural changes identified here are associated with mTBI vs. with typical aging. Nevertheless, because of our relatively short (~6-month) follow-up interval, statistical effects due to typical aging are likely much weaker than those due to TBI [46–49]. For this reason, the FA changes reported here are likely due primarily to TBI and typical aging effects would be relatively minor by comparison. This assertion is strongly supported by the existing body of literature on this topic, as elaborated below.

Upon quantifying WM changes in HCs aged 21 to 49 y ($\mu \pm \sigma = 27 \pm 7$ y) across 3–5 months, Mayer et al. [50] found no statistically significant FA changes in the left superior corona radiata, left UF, left internal capsule, left corona radiata, GCC, or SCC. In the SCC, we found TBI-related mean FA changes with Cohen's $d = 0.24$ (Table 2). By contrast, Mayer et al. found an effect size of 0.05 in this structure across a comparable interval. In a study replicating that of Mayer et al., Ling et al. [51] found, unexpectedly to us, mean FA *increases* in the CCs of HCs, rather than *decreases* as found here in TBI participants. Partly because the sample of Ling et al. included adult HCs, these authors proposed that head motion—rather than natural aging—accounted for the FA increases they identified.

Across ~6 months, Lancaster et al. [52] found no significant diffusion tensor imaging-derived diffusivity changes in HCs aged 18–20 y ($\mu \pm \sigma = 20 \pm 2$ y). Although these authors quantified radial and axial diffusivities rather than FA, their findings likely parallel ours due to the algebraic relationship between these three variables [53]. In HCs, like Mayer et al., Lancaster et al. found an axial diffusivity *increase* in the BCC as a function of increasing age. Similarly, Vik et al. [54] found an FA *increase* in the left CSTs of

HCs aged 52–66 y ($\mu \pm \sigma = 59 \pm 7$ y) and imaged across 3–4 years, whereas we found an FA *decrease*. Finally, Yin et al. [55] quantified WM changes in HCs aged 26–50 ($\mu \pm \sigma = 38 \pm 12$ y) and found no effect (Cohen's $d = 0$) associated with FA change in the BCC. This is in contrast with our effect size of $d = 0.29$ associated with FA decrease in TBI participants (Table 2).

In summary, previous studies found either very small increases or no change in callosal mean FA among HCs, whereas we found moderate FA decreases among TBI participants across comparable time intervals. Other studies' findings of very small FA increase in HCs are incompatible with natural aging effects on callosal WM (whose mean FA decreases with age), such that the increases in question are likely artifactual [51]. This may indicate that in HCs, across a ~6-month period, aging effects on mean FA may be comparable to those of DWI motion artifacts, such that detecting the former could be very challenging. Nevertheless, we acknowledge that our lack of a reference sample is a limitation of this study.

As individuals age, they accumulate multiple pathologies related not only to typical aging but also to processes related to Alzheimer's disease, neurovascular disease, and/or to proteinopathies involved in other clinical conditions. For this reason, the WM degradation quantified in this study is likely due not only to TBI but also, at least in part, to non-traumatic processes. Because such processes can interact with TBI, the statistical associations identified here may be multifactorial rather than associated with TBI alone. Nevertheless, as already stated, previous studies of older control participants without TBI found hardly any WM degradation over the follow-up period of our study. The longer temporal course associated with typical aging supports the interpretation that TBI is the predominant cause of the WM degradation quantified here over ~6 months.

Abbreviations BCC: Body of the corpus callosum; CC: Corpus callosum; CI: Confidence interval; CMB: Cerebral microbleed; CST: Corticospinal tract; DWI: Diffusion-weighted imaging; FA: Fractional anisotropy; GCC: Genu of the corpus callosum; GCS: Glasgow Coma Scale; GM: Gray matter; ILF: Inferior longitudinal fasciculus; IOFF: Inferior occipitofrontal fasciculus; MdLF: Middle longitudinal fasciculus; mTBI: Mild traumatic brain injury; PC: Principal component; PCA: Principal component analysis; SCC: Splenium of the corpus callosum; Sup-F: Superficial frontal; Sup-P: Superficial parietal; Sup-T: Superficial temporal; SWI: Susceptibility-weighted

imaging; TBI: Traumatic brain injury **Acknowledgements** The authors are thankful to study participants and to Alexander S. Maher for his editorial assistance.

Author contribution Authors contributed to study design (D.J.R., D.J.O., H.C.C., A.I.), participant recruitment (L.G., A.I.), data analysis (D.J.R., A.D., K.A.R., N.N.C., V.N., F.Z.), result interpretation (D.J.R., A.D., L.G., N.S.-B., H.C.C., A.I.), and manuscript redaction (D.J.R., A.D., N.S.-B., H.C.C., A.I.).

Funding This work was supported by the National Institutes of Health (grant R01 NS 100973 to A.I.), by the Department of Defense (award W81-XWH-1810413 to A.I.), by a grant from the James J. and Sue Femino Foundation to A.I., by a Hanson-Thorell Research Scholarship to A.I., by the Undergraduate Research Associate Program (URAP) at the University of Southern California, and by the Center for Undergraduate Research in Viterbi Engineering (CURVE) at the University of Southern California. L.J.O. and F.Z. acknowledge funding from the National Institutes of Health, including the National Institute of Biomedical Imaging and Bioengineering (grants P41 EB 015902, P41 EB 015898, P41 EB 028741) and the National Institute of Mental Health (grants R01 MH 074794, R01 MH 125860, and R01 MH 119222).

Data availability Primary data generated and/or analyzed during the current study are available subject to a data transfer agreement. At the request of some participants, their written permission is additionally required in some cases.

Code availability Programming code developed and used for the study is available from the corresponding author subject to an intellectual property agreement.

Declarations

Ethics approval This study was undertaken in adherence to the US Code of Federal Regulations (45 CFR 46) and with approval from the Institutional Review Board at the University of Southern California.

Consent to participate All participants provided written informed consent.

Consent for publication All authors provided their consent to publish this study in its current form.

Competing interests The authors declare no competing interests.

References

1. Rockhill CM, et al. Health care costs associated with traumatic brain injury and psychiatric illness in adults. *J Neurotrauma*. 2012;29(6):1038–46.

2. Taylor CA, et al. Traumatic brain injury-related emergency department visits, hospitalizations, and deaths – United States, 2007 and 2013. *MMWR Surveill Summ.* 2017;66(9):1–16.
3. Biswas RK, Kabir E, King R. Effect of sex and age on traumatic brain injury: a geographical comparative study. *Arch Public Health.* 2017;75:43.
4. Marquez de la Plata CD, et al. Impact of age on long-term recovery from traumatic brain injury. *Arch Phys Med Rehabil.* 2008;89(5):896–903.
5. Testa JA, et al. Outcome after traumatic brain injury: effects of aging on recovery. *Arch Phys Med Rehabil.* 2005;86(9):1815–23.
6. Najem D, et al. Traumatic brain injury: classification, models, and markers. *Biochem Cell Biol.* 2018;96(4):391–406.
7. Skandsen T, et al. Incidence of mild traumatic brain injury: a prospective hospital, emergency room and general practitioner-based study. *Front Neurol.* 2019;10:638.
8. Freeze WM, et al. Blood–brain barrier leakage and microvascular lesions in cerebral amyloid angiopathy. *Stroke.* 2019;50(2):328–35.
9. Rostovsky KA, Maher AS, Irimia A. Macroscale white matter alterations due to traumatic cerebral microhemorrhages are revealed by diffusion tensor imaging. *Front Neurol.* 2018;9:948.
10. Liao R, et al. Performance of unscented Kalman filter tractography in edema: analysis of the two-tensor model. *Neuroimage Clin.* 2017;15:819–31.
11. Zhang F, et al. An anatomically curated fiber clustering white matter atlas for consistent white matter tract parcellation across the lifespan. *Neuroimage.* 2018;179:429–47.
12. Jolliffe IT. Discarding variables in a principal component analysis. I: artificial data. *Appl Stat Ser C.* 1972;21(2):160–73.
13. Jolliffe IT. Discarding variables in a principal component analysis. II: real data. *Appl Stat Ser C.* 1973;22(1):21–31.
14. Irimia, A, Bradshaw, LA. Ellipsoidal electrogastrographic forward modelling. *Physics Med Biol.* 2005; 50(18):4429.
15. Tremblay S, et al. Diffuse white matter tract abnormalities in clinically normal ageing retired athletes with a history of sports-related concussions. *Brain.* 2014;137(Pt 11):2997–3011.
16. Liu H, et al. Aging of cerebral white matter. *Ageing Res Rev.* 2017;34:64–76.
17. Tremblay S, et al. Mild traumatic brain injury: the effect of age at trauma onset on brain structure integrity. *Neuroimage Clin.* 2019;23:101907.
18. Gardner A, et al. A systematic review of diffusion tensor imaging findings in sports-related concussion. *J Neurotrauma.* 2012;29(16):2521–38.
19. Stamm JM, et al. Age at first exposure to football is associated with altered corpus callosum white matter microstructure in former professional football players. *J Neurotrauma.* 2015;32(22):1768–76.
20. Trotter BB, et al. Military blast exposure, ageing and white matter integrity. *Brain.* 2015;138(Pt 8):2278–92.
21. Irimia, A, Van Horn, JD. Functional neuroimaging of traumatic brain injury: advances and clinical utility. *Neuropsychiatr Dis Treat.* 2011;11:2355.
22. Irimia, A, Torgerson, CM, Goh, SYM, Van Horn, JD. Statistical estimation of physiological brain age as a descriptor of senescence rate during adulthood. *Brain Imaging Behav.* 2015;9(4):678–689.
23. Halgren E, Sherfey JS, Irimia A, Dale AM, Marinkovic K. Sequential temporo-fronto-temporal activation during monitoring of the auditory environment for temporal patterns. *Human Brain Mapping.* 2011;32(8):1260.
24. Caeyenberghs K, et al. Bimanual coordination and corpus callosum microstructure in young adults with traumatic brain injury: a diffusion tensor imaging study. *J Neurotrauma.* 2011;28(6):897–913.
25. Ewing-Cobbs L, et al. Corpus callosum diffusion anisotropy correlates with neuropsychological outcomes in twins discordant for traumatic brain injury. *AJNR Am J Neuroradiol.* 2006;27(4):879–81.
26. Funnell MG, Corballis PM, Gazzaniga MS. Insights into the functional specificity of the human corpus callosum. *Brain.* 2000;123(5):920–6.
27. Ota M, et al. Age-related degeneration of corpus callosum measured with diffusion tensor imaging. *NeuroImage.* 2006; 31(4).
28. Stojanovski S, et al. Microstructural abnormalities in deep and superficial white matter in youths with mild traumatic brain injury. *NeuroImage Clin.* 2019; 24.
29. Phillips OR, et al. Superficial white matter: effects of age, sex, and hemisphere. *Brain Connect.* 2013;3(2):146–59.
30. Herbet G, Moritz-Gasser S, Duffau H. Direct evidence for the contributive role of the right inferior fronto-occipital fasciculus in non-verbal semantic cognition. *Brain Struct Funct.* 2017;222(4):1597–610.
31. Goldstein FC, Levin HS. Cognitive outcome after mild and moderate traumatic brain injury in older adults. *J Clin Exp Neuropsychol.* 2001;23(6):739–53.
32. Nazeri A, et al. Superficial white matter as a novel substrate of age-related cognitive decline. *Neurobiol Aging.* 2015;36(6).
33. Bazarian JJ, et al. Sex differences in outcome after mild traumatic brain injury. *J Neurotrauma.* 2010;27(3):527–39.
34. Fakhran S, et al. Sex differences in white matter abnormalities after mild traumatic brain injury: localization and correlation with outcome. *Radiology.* 2014;272:815–23.
35. Han Z, et al. White matter structural connectivity underlying semantic processing: evidence from brain damaged patients. *Brain.* 2013;136(Pt 10).
36. Lawrence TP, et al. Early detection of cerebral microbleeds following traumatic brain injury using MRI in the hyper-acute phase. *Neurosci Lett.* 2017;655:143–50.
37. Gyanwali B, et al. Mixed-location cerebral microbleeds: an imaging biomarker for cerebrovascular pathology in cognitive impairment and dementia in a memory clinic population. *J Alzheimers Dis.* 2019;71(4):1309–20.
38. Reeves TM, Phillips LL, Povlishock JT. Myelinated and unmyelinated axons of the corpus callosum differ in vulnerability and functional recovery following traumatic brain injury. *Exp Neurol.* 2005;196(1).
39. Bigler E, et al. The temporal stem in traumatic brain injury: preliminary findings. *Brain Imaging Behav.* 2010;4(3):270–82.

40. Conta A, Stelzner D. Differential vulnerability of propriospinal tract neurons to spinal cord contusion injury. *J Comp Neurol*. 2004;479:347–59.
41. Makris N, et al. Human middle longitudinal fascicle: segregation and behavioral-clinical implications of two distinct fiber connections linking temporal pole and superior temporal gyrus with the angular gyrus or superior parietal lobule using multi-tensor tractography. *Brain Imaging Behav*. 2013;7(3):335–52.
42. Makris N, et al. Mapping temporo-parietal and temporo-occipital cortico-cortical connections of the human middle longitudinal fascicle in subject-specific, probabilistic, and stereotaxic Talairach spaces. *Brain Imaging Behav*. 2017;11(5):1258–77.
43. Shimizu Y, Sakai KL. Visualization of gray matter myelin and fiber bundles critical for relative pitch: a role of the left posterior long insular cortex. *Brain Nerve*. 2015;67(9):1147–55.
44. Bartzokis G. Age-related myelin breakdown: a developmental model of cognitive decline and Alzheimer's disease. *Neurobiol Aging*. 2004; 25(1).
45. Butt AM, Berry M. Oligodendrocytes and the control of myelination in vivo: new insights from the rat anterior medullary velum. *J Neurosci Res*. 2000;59(4).
46. Edlow BL, et al. Diffusion tensor imaging in acute-to-sub-acute traumatic brain injury: a longitudinal analysis. *BMC Neurol*. 2016;16(1):2.
47. Ling JM, et al. Biomarkers of increased diffusion anisotropy in semi-acute mild traumatic brain injury: a longitudinal perspective. *Brain*. 2012;135(Pt 4).
48. Newcombe V, et al. Dynamic changes in white matter abnormalities correlate with late improvement and deterioration following TBI: a diffusion tensor imaging study. *Neurorehabil Neural Repair*. 2016;30(1).
49. Patel JB, et al. Structural and volumetric brain MRI findings in mild traumatic brain injury. *Am J Neuroradiol*. 2020;41(1):92.
50. Mayer AR, et al. Functional connectivity in mild traumatic brain injury. *Hum Brain Mapp*. 2011;32(11):1825–35.
51. Ling J, et al. Head injury or head motion? Assessment and quantification of motion artifacts in diffusion tensor imaging studies. *Hum Brain Mapp*. 2012;33(1):50–62.
52. Lancaster MA, et al. Chronic differences in white matter integrity following sport-related concussion as measured by diffusion MRI: 6-month follow-up. *Hum Brain Mapp*. 2018;39(11):4276–89.
53. Winklewski PJ, et al. Understanding the physiopathology behind axial and radial diffusivity changes – what do we know? *Front Neurol*. 2018;9:92.
54. Vik A, et al. Fractional anisotropy shows differential reduction in frontal-subcortical fiber bundles – a longitudinal MRI study of 76 middle-aged and older adults. *Front Aging Neurosci*. 2015;7:81.
55. Yin B, et al. Longitudinal changes in diffusion tensor imaging following mild traumatic brain injury and correlation with outcome. *Front Neural Circuits*. 2019;13:28.

Publisher's note Springer Nature remains neutral with regard to jurisdictional claims in published maps and institutional affiliations.